DRUG-LOADED HYDROGEL WOUND INFECTION THERAPIES

TREATMENT OF OPEN WOUND INFECTIONS USING DRUG-IMPREGNATED POLYMER HYDROGELS: A DUAL APPROACH

By JODY C. MOHAMMED, B.SC.

A Thesis Submitted to the School of Graduate Studies in Partial Fulfilment of the Requirements for the Degree Master of Science

McMaster University MASTER OF SCIENCE (2022) Hamilton, Ontario (Chemical Biology)

TITLE: Treatment of Open Wound Infections Using Drug-Impregnated Polymer Hydrogels: A Dual Approach AUTHOR: Jody C. Mohammed, B.Sc. (Cornell University) SUPERVISOR: Dr. Brian K. Coombes NUMBER OF PAGES: ix, 50

LAY ABSTRACT

Open wounds are breeding grounds for infection and can pose severe threats to individuals with compromised immune systems and other at-risk groups. Antibiotic-resistant bacteria thrive in these polymicrobial environments and are often difficult to treat. In tandem, challenges in the drug discovery pipeline lead to slow development of new antibiotics and routes of administration. One such challenge is the issue of solubility of drug compounds. Otherwise promising drugs face hurdles in administration due to their poor water solubility. These barriers highlight the need for unconventional approaches to drug discovery and the delivery of therapeutics. In collaboration with an Edmonton-based biotechnology company and other research groups at McMaster University, we studied two novel hydrogels loaded with antibiotics of interest to address the aforementioned challenges in treating infected wounds. Utilizing patented technology and pre-clinical animal models, the two proposed routes of antibiotic administration show promise in delivering drugs with inherently low water solubility and offer several other advantages in the development of efficient drug delivery vehicles.

ABSTRACT

The skin is the body's largest organ and serves a variety of essential functional and aesthetic purposes. Wounds, burns, and other abrasions to the skin can have consequential effects on the rest of the body if not properly managed. Open wounds are often a breeding ground for bacterial infections and can pose a severe threat to individuals with compromised immune systems and other at-risk groups. Antibiotic-resistant bacteria, such as methicillin-resistant *Staphylococcus aureus* (MRSA), thrive in these polymicrobial environments and are often difficult to treat. In tandem, bottlenecks in the drug discovery pipeline lead to slow development of novel compounds and routes of administration. One such challenge is the inherent issue of solubility of antibiotic compounds. Otherwise promising drug candidates face challenges in administration in critical cases, such as open wounds, due to their poor aqueous solubility. These barriers highlight the need for unconventional approaches to drug discovery and the delivery of therapeutics. In collaboration with an Edmonton-based biotechnology company and other research groups at McMaster University, we performed a comparative analysis of two novel hydrogels loaded with antibiotics of interest to address the aforementioned challenges in treating infected wounds. Utilizing patented technology and an optimized excisional murine wound model, the two proposed routes of antibiotic administration show promise in delivering drugs with inherently low water solubility and offer several other advantages in the development of efficient drug delivery vehicles.

ACKNOWLEDGEMENTS

I would like to thank my supervisor Dr. Brian Coombes for supporting and advocating for me from the get-go. My success at McMaster would not have been possible without your open-mindedness and trust in me and my unique path through science and academia. You helped me build upon my skills as an engineer and flourish in the world of science. Thank you to my committee members Dr. Todd Hoare and Dr. Lori Burrows for your continued support and patience as I navigated the process of constructing the story that is my thesis. Having mentors that represent success in various fields has kept me keen to delve into the future with an open mind. To the growing list of collaborators involved in this project, you have been a pleasure to work with and learn from during the last two years. To my mentor during my undergraduate years, Dr. Aravind Natarajan, you are one of the main reasons I am where I am today. Your passion not only for science, but inspiring it in others, has kept me driven to be and do the same.

To the friends I have made in and out of the Coombes lab during the past two years – you have kept me not only grounded, but genuinely happy during what was an otherwise tough period for us all as a whole. I couldn't have done any of this without your unwavering encouragement and friendship. Lastly, thank you to my family: Mama, Papa, Ridley, and Snoopy. Together we have navigated the world; but you all have also been instrumental in helping me navigate my academic career. Each one of you has provided insurmountable support over the last several years and I cannot thank you enough. You are the three most inspiring people (and single most inspiring dog) I know. I love you all so much and once again, would not be where I am today without you.

Table of Contents

List of Figures and Tables

List of All Abbreviations and Symbols

AMR – Antimicrobial resistance
BSA – Bovine serum albumin
CFU – Colony forming unit
CIJM – Confined impinging jet mixer
CP – Cyclophosphamide
ESI – Electrospray ionization
ESKAPE – Enterococcus faecium, Staphylococcus aureus, Klebsiella pneumoniae, Acinetobacter baumannii, Pseudomonas aeruginosa, Escherichia coli,
FA – Fusidic acid
FA/AZT – Fusidic acid and Azidothymidine
HPLC – High-performance liquid chromatography
iPX – Impregnated, pressurized, and expanded
LB – Luria broth
LC-MS – Liquid chromatography-mass spectrometry
MIC – Minimum inhibitory concentration
MRSA – Methicillin-resistant *Staphylococcus aureus*
OD_{600} – Optical density at 600 nanometers
OX – Oxacillin
PBS – Phosphate buffered saline
PEG – Polyethylene glycol
PGX – Pressurized Gas eXpanded
PGX-SA – Pressurized Gas eXpanded sodium alginate
POEGMA – Poly(oligoethylene glycol methacrylate)
SA – Sodium alginate
SAP – self-assembled particles
S. aureus – Staphylococcus aureus
SC-AP – Supercritical, adsorptive precipitation
SC-CO_2 – Supercritical carbon dioxide
SEM – Standard error of the mean
SWF – Simulated wound fluid
TIG – Tigecycline
SF – Sodium fusidate
TS – Thiostrepton
xSA – Crosslinked sodium alginate

Declaration of Academic Achievement

Jody C. Mohammed (JCM), Dr. Brian K. Coombes (BKC), and Aline Fiebig designed experiments; JCM performed experiments, conducted animal studies, and analyzed data; Lena Darwish aided in animal experiments; Dr. Byron Yepez fabricated PGX materials and performed SC-AP drug impregnations; Ridhdhi Dave synthesized POEGMA polymers; JCM fabricated POEGMA nanoparticles; Samaneh Toufanian generated POEGMA gels; Dr. Tracey Campbell, Catherine Luck, and Nicola Henriquez performed drug quantification studies.

Introduction

Skin wound infections

Skin wounds and abrasions are common in all areas of the world and health care system. Wounds are non-specific ailments that vary in size, shape, cause, and consequence[1,2]. Moreover, infection of wounds with a pathogen or combination of pathogens compromises the body's normal wound-healing process[3,4,5]. For these reasons, wound care has drawn increased focus in many areas of research. Recent advancements include nanomaterials, plant-derived products, negative pressure wound therapies, and several others[6–8]. However, only a select few address the specific need for infection-management therapies, such as nanomaterial-based products and topical antimicrobial formulations[6,9]. Although significant work has been done in the understanding of wound infections and the development of therapies, the incidence and cost of compromised wounds continues to rise worldwide[10].

The cost of wound care goes beyond just financial ramifications; the prevalence and variability of wound infections results in constant personal, clinical, and financial distress[11]. Acute and chronic wound infections are widespread burdens on individuals of all ages, ethnicities, and socioeconomic backgrounds. Hospital intensive care wards report some of the highest rates of infected wounds globally, causing increased concern for patients likely in already immunocompromising conditions[12]. Additionally, upwards of 40% of all hospital inpatients have reported wounds, 7.3% of which are compromised with an active infection[13]. This has led the global cost of wound care to surpass $17 billion in 2021, with an expected increase to $28 billion annually by 2029[14].

The antimicrobial resistance crisis

The growing antimicrobial resistance (AMR) crisis is one of the key reasons that compromised wounds and therapeutic advancements in their treatment will only become more critical with time[14]. It is estimated that over 700,000 deaths annually are due to infections by drug-resistant pathogens[15]. The World Health Organization has assigned critical priority status for research and development to six pathogens known as the *ESKAPE* group[16]. Due to their already high and increasing levels of AMR, *Enterococcus faecium, Staphylococcus aureus, Klebsiella pneumoniae, Acinetobacter baumannii, Pseudomonas aeruginosa,* and *Escherichia coli* are now a key focus in global research for new preventative and anti-infective strategies[16]. Several of these pathogens are commonly found in compromised and infected wounds, drawing more interest and resources to the wound care market in recent years[14].

Methicillin-resistant Staphylococcus aureus

Staphylococcus aureus and other *ESKAPE* pathogens continue to be detrimental players in skin wound infections worldwide[17]. Genomic mutations and horizontal gene transfer have led to the spread of antibiotic-resistance genes among these bacteria[18]. One such resistance gene is *mecA,* found in many common strains of *Staphylococcus aureus*[19]. Although denoted methicillin-resistant *Staphylococcus aureus* (MRSA), this pathogen encodes resistance to several other classes of common antibiotics in addition to methicillin[20]. Since their discovery in 1961, MRSA isolates have continued to display decreasing levels of susceptibility to previously successful antibiotic compounds[20]. This

has led MRSA to be among the key public health concerns as a cause of community and hospital-acquired infections. Unfortunately, some of the most promising drugs in combatting infections by these bacteria are compounds that suffer from difficulties in administration. Whether a drug is unsuccessful at its investigational stages or has inherent complications in formulation, many potential therapeutics fail to make it to market. This only reinforces the need for new approaches in antibiotic discovery and administration.

Low drug solubility and other therapeutic challenges

In addition to concerning levels of AMR progression, some common therapeutic options, such as topical silver agents, have proven insufficient. Recent meta-analyses reveal a poor correlation between traditional silver dressings and bacterial load, as well as the success of these products in preventing infection in wounds[21]. These setbacks highlight the need for either new antibiotic candidates or novel methods of anti-infective delivery. However, in developing new drug compounds, many inherent chemical and physical challenges lead to complications in the formulation steps required to ensure the safety and stability of a drug[22]. These characteristics can severely limit administration efficacy and often require additional formulation steps to overcome the challenges they present.

Low aqueous solubility is one of the most prevalent and critical issues faced by potential antibiotic compounds in the drug discovery pipeline. Over 40% of newly generated compounds in the pharmaceutical industry are largely water-insoluble[22]. This results in questionable antibiotic candidacy of a drug, as bioavailability is often directly

related to the solubility of a compound[22]. As a result, there has been extensive work done to understand and manage inherently low water solubility. Several strategies have been proposed to address these complications, including the addition of surfactants or co-crystals, or altering particle size and binding morphologies[23]. However, these techniques are often slow, expensive, or require additives that compromise the safety and/or stability of the drug. Compound solubility is therefore one of the most frequent, yet addressable bottlenecks in the wound care market, and the main hurdle attempted to overcome with this project.

Fusidic acid (FA) is an antibiotic produced by a strain of *Fusidium* fungus and has activity against *S. aureus* and other Gram-positive pathogens[24]. FA has low toxicity, minimal resistance levels, and shows no cross-resistance with other antibiotics, making it an ideal candidate for therapeutic use in MRSA infections[25]. Unfortunately, FA is only sparingly soluble in aqueous medias, making formulation of the compound challenging[24].

Tigecycline (TIG), a recently developed compound with excellent bioavailability, belongs to the tetracycline class[26]. It has drawn significant attention in the last two decades as a front-runner of a new generation of drugs known as the glycylcyclines[27]. Several formulations of TIG have been evaluated in attempts to exploit its broad-spectrum activity and low levels of resistance[28,29–32]. Nimal *et al.* demonstrated the use of TIG in injectable, chitosan-PRP hydrogels, while Sakarya *et al.* demonstrated the success of topical TIG penetration into the ocular humor and cornea[32,33]. However, there is more work needed to confirm TIG's promise as a broad-spectrum antibiotic for skin infections. Its limited aqueous solubility has arisen as a barrier to during formulation in many

cases[34,35]. For these reasons, we selected FA and TIG as the first bioactives to test with the technologies presented in this report.

Pressurized, gas-expanded liquids

Polymer processing and loading has recently gained popularity as a drug carrying and delivery method due to its tunability and efficiency[36]. More specifically, the previously mentioned insoluble therapeutic compounds are ideal candidates for this type of nano-dispersion and deposition-based delivery vehicle. While the range of strategies investigated in attempts to overcome drug solubility issues is broad, polymeric bio-aerogels and other highly porous structures continue to be frontrunners in terms of efficiency, tunability and stability.

A team of researchers at Ceapro Inc. optimized the Pressurized Gas eXpanded Liquid (PGX) technology invented by Temelli and Seifried to generate aerogels which can be used as macroporous polymeric scaffolds for drug delivery[37]. The process involves pumping and mixing a sodium alginate (SA) slurry with the PGX liquid, which consists of supercritical CO_2 (SC-CO_2) and ethanol, to rapidly dehydrate and precipitate the SA. Once precipitated, a purified and dried fibrous aerogel (PGX-SA) is generated[38]. The resulting PGX-SA can be used as scaffolds for further steps. This technology offers significant advantages over conventional SA processing methods because it generates open, porous particles, increases the specific surface area and water-binding capacity while simultaneously allowing control over the internal pore sizes[38]. Work by the Hoare Lab (McMaster University, Department of Chemical Engineering) and Ceapro's research

team has demonstrated the crosslinking potential of the PGX base material and characterized the physicochemical properties of the material via mechanical studies.

Supercritical adsorptive precipitation

Supercritical fluid impregnation of bioactive compounds has become a common method of generating controlled drug delivery products[39]. Alternative 'impregnation' methods with similar loading and delivery mechanics often face hurdles in the context of insoluble compounds. And thus, the ability to efficiently load bioactive compounds into the PGX-SA scaffolds is the basis for the second in-house process utilized by Ceapro Inc.

To avoid the use of organic solvents that are undesirable in applications intended for human use and to achieve homogenous drug loading, supercritical adsorptive precipitation (SC-AP) using SC-CO_2 can be used to load insoluble compounds onto PGX-SA. The process consists of solubilizing the drug of choice in SC-CO_2 at a specified temperature and pressure. The solubilized compound is then circulated through the pores of the PGX-SA material where a portion is adsorbed into the internal and external surface area of the polymer scaffolds. Finally, upon depressurization of the vessel, the SC-CO_2 loses its solvent capabilities and the remaining drug precipitates onto the exterior surfaces of the PGX-SA material[40]. Most importantly, SC-CO_2's mild operating temperature, only slightly higher than room temperature, preserves the stability and activity of heat-labile compounds during the SC-AP process.

Poly(oligoethylene glycol methacrylate) self-assembled nanoparticles and hydrogels

Water-based hydrogels are another widely used form of controlled drug delivery and release[41]. However, limitations in control over the gelling mechanics and loading quantities are often encountered with traditional polymer-based hydrogels such as poly(ethylene glycol) (PEG). Specifically, the high-water content associated with these products results in an inability to reach therapeutic-level doses of hydrophobic drugs. Extensive chemical modifications are frequently necessary to induce and sustain hydrogel formation by these polymers, leading to stability and toxicity concerns[42]. Additionally, development of stable formulation of the non-soluble drugs that are to be introduced to these matrices requires unique approaches for efficient loading and release.

To address these concerns and offer a novel route of antibiotic delivery into wounds, the Hoare Lab developed an in-house, bench-top system of synthesizing drug-encapsulated nanoparticles loaded into a tunable, water-based hydrogel. Poly(oligoethylene glycol methacrylate) (POEGMA) is a brush polymer analogue of PEG that can be functionalized via copolymerization[7]. The compound of interest is encapsulated by POEGMA brush polymers that self-assemble via a flash nanoprecipitation mechanism. Hydrazide- and aldehyde-functionalized POEGMA precursors are then combined with the nanoparticles for *in situ* gelation in pre-cut silicone molds. The functionality of the POEGMA precursors allow for extensive tunability in gelation kinetics and many other chemical and physical properties[43]. Additionally, the polymer network's adhesion capabilities allow for easy removal from mucous- or

exudate-containing environments, such as wound beds, and they are an attractive option for antibiotic administration to compromised sites[43].

Full-thickness excisional murine wound model

A critical aspect of developing any new therapeutic candidate is analyzing its effectiveness and safety using animal models. The model should emphasize clinical relevancy, follow all ethical standards, and be reliably reproducible. For this study, a full-thickness skin wound model was developed and carefully optimized to meet the above criteria.

Cyclophosphamide (CP) is a widely used agent that results in neutrophil depletion and T cell inactivation in mice[44]. These conditions are often necessary for high-throughput and in-depth evaluation of infective disease progression in murine models. This is, in part, due to the opportunistic nature of many infectious agents[45]. To evaluate these opportunistic pathogens in animal models, inducing relevant immunocompromising conditions is necessary. However, the side effects associated with the administration of CP in mice can also result in unwanted experimental conditions in some cases. Specifically, in the case of infected wound models, neutropenia results in significant weight loss in experimental animals, making weight loss due to infection more difficult to monitor. Moreover, neutropenia is not a clinically relevant condition in all wound infection cases. Patients with immunocompromising ailments may be optimally modeled with CP induction, but the condition cannot be assumed widely relevant. Although the

use of CP is sometimes necessary in the modeling of bacterial infections, more work needs to be done to examine the necessity of CP induction in specific cases[46].

In this study, a full-thickness, excisional wound model was used to examine the effectiveness of the iPX and POEGMA agents *in vivo*. Murine wound models offer excellent insight into the body's natural wound healing capabilities. However, due to the rodent's confounding wound contraction mechanisms, skin abrasions need a secondary method of wound bed reinforcement for clinical modeling in mice. Sterile plastic washers are used to keep murine wound models from undergoing their natural contraction process[47].

Current standards of care for wound infections

As mentioned, shortcomings of several widely used wound care products, such as silver dressings, have been identified in recent years[21]. The lack of thorough clinical trials, high production costs, and fabrication sustainability are just some of the considerations making silver-based wound dressings less desireable[48]. Therefore, there has been a shift in focus in advanced wound care products. Therapies such as hydrogels have quickly become a standard of care for the management of complicated, infected wounds. The biocompatibility, swelling/water content, and tunability of both natural and synthetic hydrogels make them favored options in infection therapy[41]. Many hydrogel products have advantages and properties beyond just bioactive delivery[49,50,51,52]. Song *et al.* generated cell-adhering, polypeptide hydrogels with inherent antibacterial activity

against *E. coli* and *S. aureus* strains[52]. These novel wound-healing scaffolds are just one of the many recent and promising developments in the wound care market.

However, the water-based nature of many of these products narrows the list of deliverable compounds to those having at least moderate aqueous solubility. Limitations in efficiently preparing then delivering bioactives from hydrogels arise when the drug of interest has low inherent aqueous solubility. The drug-loading mechanisms of both technologies/products presented in this report overcome this issue in that they both efficiently carry and distribute insoluble drug compounds to infected wound sites.

Hypothesis

Due to the complexity and variability of wound bed infections as well as the lack of tunable, highly-efficient advanced wound treatment options, we suggest that **drug-impregnated iPX disks and POEGMA gels offer a useful route of antibiotic administration into compromised wound sites.**

Results

Cyclophosphamide is not required to establish MRSA infection in murine skin wound model.

Previous work suggested the need to induce neutropenia and other immune deficiencies in mice using cyclophosphamide (CP) to establish infection. To determine whether CP induction was a necessary step in the model used for this work, we examined its effect on weight loss, bacterial infection establishment, and overall well-being of

experimental animals. Mice were treated twice with CP at 4- and 1-day pre-infection and compared with a non-treated control group. Both groups were inoculated with ~$5x10^6$ colony forming units (CFU) of MRSA and housed for 24 hr prior to assessment. Post-infection tissue sample results in **Figure 2** suggest the successful establishment of a MRSA infection in the wound bed in both CP pre-treated and non-treated groups. Moreover, weight loss and morbidity in CP pre-treated mice was critically higher than non-treated mice (**Figure 2**). Together, these data suggest that CP is dispensable as a pre-treatment for MRSA (strain USA 300) infection in a full-thickness, murine skin wound model.

iPX disks are sufficiently and uniformly loaded with FA.

High-performance liquid chromatography (HPLC) and mass spectrometry (MS) were used to separate the components of the disks from the bioactives. These analyses suggested the FA-iPX disks (average mass: 4.2 mg) are loaded with an average of 5.1 μg (SD: 0.46) FA each (**Figure 6**).

***In vitro* tests show successful loading and deposition of antibiotic compounds by iPX disks and POEGMA gels.**

Disk diffusion assays were used to assess loading and release efficiency of the drug-impregnated disks and gels. The various treatment options were placed on Luria broth (LB)-agar plates inoculated with MRSA in minimum triplicate counts along with control disks for 16-18 hr. FA and TIG-impregnated iPX disks both demonstrated

comparable inhibition zones: FA-iPX disks had an average 27.2 mm clearance diameter and TIG-iPX disks had an average 24.0 mm diameter (**Figure 3**). FA-POEGMA gels displayed an average of 30.3 mm diameter of inhibition in comparison to control gels, indicating a suppression of bacterial growth in these areas (**Figure 3**).

iPX disks impregnated with fusidic acid prevent MRSA expansion in murine wound model.

Fusidic acid's solubility issues in administration and therapeutic development make it an ideal candidate for use in the iPX technologies and products. The full-thickness skin wound model described below was used to evaluate FA-iPX disks as drug delivery vehicles in compromised wounds. FA, a bacteriostatic compound, was impregnated into PGX disks using the SC-AP technology and introduced into the infected wounds. Treatment disks were placed in wound beds 1 hr post-infection (~$5x10^6$ CFU inoculum) and left to deposit drug for 48 hr. Retention of inoculum-level bacterial counts post-infection (48 hr) suggests iPX disks are successful in delivering loaded FA and preventing expansion of MRSA colonization in the wounds. FA-iPX treated mice experienced no increase in bacterial CFU between the time of infection and the time of sacrifice, in comparison to untreated mice that experienced a significant increase in bacterial CFU by 1-2 orders of magnitude during the same timeframe. Mice treated with control iPX disks (no compound) had slightly reduced level of bacterial colonization as compared to untreated mice, though this was not significant (**Figure 4)**.

iPX disks impregnated with tigecycline eliminate MRSA infection in murine wound model.

As an initial tunability assessment of the iPX to various wound conditions, a different compound, TIG, was loaded and evaluated for wound treating potential. The full-thickness skin wound model described below was used to evaluate TIG-iPX disks as drug delivery vehicles in compromised wounds. TIG, a bacteriostatic compound that has been previously shown to exhibit bactericidal properties in certain cases[28], was impregnated into cut PGX using the SC-AP technology and introduced into the infected wounds. Treatment disks were placed in wound beds 1 hr post-infection (~$5x10^6$ CFU MRSA inoculum) and left to deposit drug for 48 hr. Total clearance of bacterial colonization post-infection (48 hr) suggests TIG-iPX disks were successful in preventing expansion of MRSA in infected wounds. TIG-iPX treated mice had no remaining bacterial CFU at the termination of the experiment, in comparison to untreated mice that experienced an increase of 1-2 orders of magnitude (from inoculum level) in CFU in the same timeframe. Mice treated with control disks (no compound) experienced an insignificant, slightly reduced level of bacterial colonization compared to untreated mice (**Figure 4**).

POEGMA gels containing FA self-assembled nanoparticles prevent MRSA expansion in murine wound model.

Previously, the POEGMA precursors have been used to generate robust, injectable hydrogels as a potential platform for both drug delivery and tissue scaffolding

applications[43]. To further explore the prospect of POEGMA and its derivatives for use in advanced wound therapeutics, POEGMA-based hydrogels were loaded with FA-containing nanoparticles. FA-containing SAPs were generated using a flash nano-precipitation mechanism and then suspended in the mixed POEGMA gel precursors. The treatment gels were placed in the surgical wound beds 1 hr post-infection (~$5x10^6$ CFU MRSA inoculum) and left to diffuse drug for 48 hr. Again, minimal expansion of inoculum bacteria during the treatment period suggests that the SAP-containing gels deliver FA and efficiently prevent MRSA infection in wounds. FA-POEGMA gel treated mice experienced no increase in bacterial CFU between the time of infection and sacrifice. Non-treated groups experienced a significant increase in CFU by 1-2 orders of magnitude during the same timeframe. Mice treated with control gels (POEGMA gels containing FA-free SAPs) experienced the same expansion in infection as the non-treated mice (**Figure 5**).

Discussion

This work demonstrates the potential of two novel wound infection therapies intended to overcome complications posed by low drug solubility, antibiotic-resistant bacteria, and compromised-wound variability. Previous studies have shown that addressing infections is the second most critical step in managing open wounds, after tissue assessment[53]. Wound healing is a complicated and time-sensitive affair, and while the body's natural healing process is impressive, assistance is often necessary. Controlled drug-delivery from wound dressings is one such method and is often favored over other

topical, medicated agents. Antimicrobials introduced via wound dressings have advantages over other methods of delivery such as less interference with the body's natural healing processes and localized activity[54]. These factors also reduce the dose of drug required, further preventing the possibility of systemic toxicity[55]. However, there are many additional factors at play when it comes to successfully delivering antimicrobial compounds to infected wound sites.

After George Winter first suggested the concept of moist wound healing, based on a study in which he witnessed more rapid epithelialization of the surrounding tissue when the wound bed was kept moist, there was a shift in focus towards hydrogel-based healing therapies[56]. Couto *et al.* recently demonstrated the ability to load bioactive compounds via supercritical adsorptive precipitation onto porous, alginate-based polymer scaffolds. The carrier/impregnation system is highly efficient both in terms of polymer processing and drug-loading. Moreover, it has the ability to carry and deliver poorly water-soluble compounds without the use of complicated or destabilizing solubilization techniques[57]. Some traditional methods of enhancing compound solubility include particle size reduction, solid dispersion, hot-melt fusions, precipitation, and the use of cryogenic technologies[58]. However, studies have shown that many, if not all, of these approaches involve physically- or chemically-degrading processing steps[59,60,61,62,63,64]. The PGX/SC-AP systems circumvent these intricacies of drug solubilization by keeping operational temperatures and pressures mild, using only food-grade solvents and processing with rapid turnaround times[40]. The resulting products are stable, uniform, and highly porous bioactive-polymer complexes that have potential application in a variety of wound

infection and other bioactive-requiring sites[57]. This study revealed the success of one such application: delivery of insoluble drug compounds to open and infected wound sites.

When Lutz *et al.* further characterized and made popular the work done to develop PEG-analogue block polymers based on poly(oligoethylene glycol methacrylate) (POEGMA) by Wang and Armes, another avenue for insoluble drug delivery became apparent[65,66]. Our study re-emphasizes this route of administration and builds upon the POEGMA precursor potential by using alternatively functionalized POEGMA monomers as hydrogel building blocks. Others have also utilized PEG-analogue block polymers to encapsulate and release bio-actives in specified locations, such as the delivery of Tat-EGFP to retinal cells by Rafat *et al.*[67]. These advancements have collectively established POEGMA as a popular basis for drug encapsulation and delivery in various fields[68]. The aldehyde- and hydrazide-functionalized POEGMA precursors have been used by the Hoare group to design hydrogels for various biomedical applications[43]. Our work expands on this by generating hydrogels containing encapsulated, insoluble compounds for *in situ* delivery into infected wound sites.

This work consists of the preliminary trials for both these technologies/products as wound infection therapeutics. As such, qualitative validation of baseline milestones, which in this case was successful loading of bioactives into the disks and gels, was necessary. This was accomplished using a series of disk diffusion (Kirby-Bauer) assays to model and evaluate the *in situ* drug release by the disks and gels in an infected environment[69]. These assays revealed that iPX disks containing FA, TIG, or the FA-AZT

combination, and POEGMA gels containing FA-SAPs were not only successfully loaded, but also loaded uniformly.

Neither the SC-AP nor POEGMA-SAP systems can load precise quantities of drug compound to individual disks or gels. While we have a rough estimate based on how much total drug was introduced into the systems and how much remained after the fabrication of the products, a secondary analysis is necessary to quantify loading amounts. To determine the level of antibiotic carried by each individual iPX disk and POEGMA gel, analyses based on dissolution of the products followed by isolation of the drug contents were used. More work is needed to characterize the drug release dynamics and swelling characteristics from both products. This will help to further clarify the dynamics of drug release, and interactions with the wound and colonizing pathogen(s)[36].

The use of infection models is an integral part of evaluating the success of novel therapeutics in the health care and biomedical fields. Previous studies reveal *in vivo* testing outperforms traditional *in vitro* studies in terms of clinical relevance and providing insight into interacting factors of host, pathogen, and antibiotic systems[70,71]. Pathogenic tolerance, susceptibility, and resistance to antibiotics is most accurately measured in live models as opposed to simulated environments[72]. In developing the wound model used for this study, we hypothesized that immunosuppression would be necessary to establish a skin infection. Previous literature defines infection establishment as little to no decrease in wound CFU from inoculum levels within the first 24 hr, with an increase in CFU providing additional evidence of infection[73]. However, when conducting a side-by-side analysis of infection progression in mice that were pre-treated with CP or

not pre-treated, both groups reached the establishment baseline in 24 hr. There was approximately a 1.1 log difference in bacterial CFU/g tissue between the two groups after 24 hr (CP pre-treated > not pre-treated). Moreover, there was a 1.66 log increase in wound CFU in the untreated mice over the course of the infection. A second consideration in deciding whether to move forward with immunosuppression in the model was whether the process resulted in unwanted side effects that impacted body condition scoring. Weight change and other measures of disease progression in experimental animals are fundamental for accurate evaluation of infection models and for detection of ethical endpoints[74]. Our study demonstrated that the weight loss and animal morbidity caused by the CP pre-treatment in BALB/c mice infringed on reliably measuring these same conditions as a result of the infection alone. Thus, CP pre-treatment was removed as a component of our wound model.

Our results demonstrate the success of FA-iPX and TIG-iPX disks in managing MRSA colonization in compromised wounds. Animals receiving blank PGX-SA disks showed a slight reduction (~0.46 log) in bacterial CFU in wound tissue as compared to the untreated group (not statistically significant). Although the reason for this has not been fully investigated, it is thought that it is, in part, due to the disk's swelling capabilities. We hypothesize that some bacteria are retained within the highly porous disk material during the infective period and are therefore removed from the wound when the disk is extracted post-mortem. It then follows that animals receiving FA-iPX disks exhibit identical or slightly reduced bacterial CFU counts to the infective inoculum size (~$5x10^6$ CFU). And although not significant, spleen CFU counts also demonstrated lower

systemic levels of infection in treated mice than untreated mice. Moreover, mice treated with FA-iPX disks lost minimal weight during the first 24 hr (average <0.5% body weight), in contrast to control groups which experienced more significant weight loss (average 3-4% body weight). However, during the second half of the infective period, FA-iPX treated mice experienced a drop in weight (average 3% body weight). We speculate this is because the FA in the disks was depleted shortly after the 24 hr mark and the remaining bacteria in the wound were able to proliferate and resume the infection progression in the mice. From these results, we concluded that the FA-loaded PGX-SA disks tested here reduce MRSA infection for at least 24 hr.

The TIG-iPX disk treatment resulted in clearing of the bacterial inoculum in its entirety. TIG's slightly higher aqueous solubility than FA, albeit still minimal (FA: 0.005 mg/mL, TIG: 0.45 mg/mL), translates to similar SC-CO_2 solubilization levels, respectively[75]. Therefore, the SC-AP stream impregnates more TIG than FA. This is likely the reason the TIG-iPX disks were more effective in clearing the MRSA inoculum and preventing infection. Minimal weight loss in treated animals in the first 24 hr (average <1% body weight) followed by weight gain (average >1% body weight) suggests that the TIG-iPX disks continue to deposit drug and ward off bacterial colonization for the length of the infective period. Lastly, the spleen CFU counts support this conclusion, as all but one experimental animal had no bacteria present in the spleen. Together, these results demonstrate not only the success of the PGX/SC-AP technologies in producing effective wound infection therapies but confirm their ability in addressing

the need for tunable and tailor-made products necessary for the treating wound infection variability.

Treatment with the POEGMA nanoparticle and hydrogel system resulted in similar therapeutic efficacy. Mice receiving FA-SAP-POEGMA gels exhibited a retention of inoculum-level MRSA counts after the 48 hr treatment period. However, in contrast to the iPX vehicle-treatment group, POEGMA vehicle-treatment animals had no drop in MRSA CFU in comparison to the untreated group. This follows our aforementioned hypothesis: the POEGMA gels are a water-based system and have little swelling capacity so they are not able to retain bacteria-containing wound fluid as the iPX disks do. Although the variance in weight loss between treated and untreated groups is not significant, mice treated with FA-SAP-POEGMA gels experienced the least weight loss. From these results, conclude that FA-SAP-containing POEGMA can prevent MRSA infection for at least 24 hr.

Future directions

To further develop the potential of drug-impregnated polymer hydrogels as an antimicrobial scaffold, the following have been recognized as necessary future steps.

(1) LC/MS quantification of TIG loading levels in iPX disks

This report includes quantification of FA levels in the first set of iPX products. To expand on the efficacy of our disks and understand the variability and interactions between different compounds and the SC-AP system, drug quantification of the TIG disks is a critical next step. After the development of a standard curve of TIG

concentrations in relevant media, LC/MS techniques will be used to extract and analyze the levels of TIG in the TIG-iPX disks.

(2) Evaluating the application of iPX disks and POEGMA gels in chronic and other long-term compromised wounds

Using a 48 hr infection model, we investigated the potential of two novel wound therapies in acute and/or short-term wound infections. To expand upon this proof of concept and broaden the possible patient pool for these products, a long-term or chronic wound model could be employed. Several research groups have successfully developed chronic wound infection models[76,77]. Re-evaluation and modulation of the treatment regime will be necessary to account for the increased length of the infection and other differences. For the iPX therapy, replacement of the disks will likely be necessary during the course of the infection. This method could then also be applied to polymicrobial infections; disks containing varying anti-infective compounds could be alternated to target any and all pathogens present, or a disk loaded with a combination of compounds could be used. For the POEGMA hydrogels, both SAP content and/or the gel's physical properties could be adjusted to control release of bioactive into the wounds. Comparative *in vivo* studies of our proposed therapeutics and the current standards of care in the wound-healing sector should be performed. Common wound-treatment approaches include topical formulations, such as ointments and creams, oral drugs and other systemic methods of antibiotic delivery, and even natural antimicrobials such as essential oils or honey. Further studies are needed to demonstrate how our proposed therapies compare to well-established options.

(3) The role of drug release kinetics from iPX and POEGMA products and the implication of wound geography

While our work demonstrates the successful delivery of antibiotic compounds to compromised wound beds, it is not yet clear how the compound progresses through the geography of the wound. It would be valuable to investigate how the infective pathogen (in this case MRSA) colonizes the wound to better understand how the bacteria and drug delivery system interact. A bioluminescent MRSA strain (such as Xen31, a derivative of ATCC 33591), coupled with fluorescent imaging, could be employed to monitor the development of infection[78]. With an understanding of where and how the inoculum colonizes in the wound, aspects of the therapeutic products or treatment regime could be adjusted to better align with the specifics of each wound. Alternatively, histological analysis of the infected wound tissue could reveal infection progression, as well as provide key insight into the body's natural immune response in these situations[73].

(4) The implications of wound-site drug release on inflammation

Another important aspect yet to be investigated is whether either of the proposed wound therapies have anti-inflammatory or otherwise adverse implications on the healing process[79]. Previous work has shown that glucocorticoid treatment impairs wound healing by suppressing the natural inflammatory stage of the wound-healing process[80]. Histological staining and examination of local and/or infected tissue could be employed to reveal inflammatory and immunological cell infiltration in those areas. BALB/c mice would be prepared with the same full-thickness, excisional wound and MRSA inoculum. Six experimental groups would be necessary to fully elucidate any off-target effects of

the therapeutics: uninfected-untreated wound, uninfected+vehicle disk, uninfected+treatment disk, infected-untreated wound, infected+vehicle disk, and infected+treatment disk.

Conclusion

The need for novel wound care technologies is intensified by (1) the rate of AMR development and (2) the failure of promising bioactive compounds due to inherent physicochemical liabilities. The variability of infected wounds further emphasizes the necessity of tunable and efficient therapeutics to target these compromised sites. Our work demonstrates the potential of two novel, drug-loaded hydrogel and bioaerogel products to address the current needs in the wound care space. Through the evaluation and characterization both iPX disks and POEGMA gels *in vitro* and *in vivo*, we suggest that these products may provide attractive options as infected-wound therapeutics.

Experimental Procedures

Preparation of bacteria

Staphylococcus aureus Rosenbach strain USA 300 was inoculated from a -80°C glycerol stock into ~5 mL LB and cultured for 16-18 h. One mL of the overnight culture was transferred into 50 mL fresh LB and allowed to subculture to stationary phase (~2.5 – 3h) or an OD_{600} = 0.4-0.6. The culture was then transferred to a 50 mL conical tube and pelleted at 4000 x g for 5 min. The supernatant was discarded and the pellet was resuspended in 10 mL PBS. This wash was repeated once more and then a 1:10 dilution

was made to measure the OD_{600} of the resuspended inoculum. The culture was then diluted to needed inoculum levels depending on the experimental procedure.

Disk diffusion assays

An overnight culture of *Staphylococcus aureus* Rosenbach strain USA 300 was grown in LB. A sterile inoculum loop was used to transfer and spread ~10 μL of bacterial culture onto prepared LB agar plates. Treatment disks were immediately placed in triplicate on plates, along with a control (blank) disk. Plates were inoculated at 37°C for 16-18 h. Zones of growth inhibition were examined and measured in anticipation of successful drug diffusion from iPX and POEGMA gels *in vivo*.

Full thickness murine skin wound model

Animal experiments were conducted according to the guidelines set by the Canadian Council on Animal Care, using protocols approved by the Animal Review Ethics Board and McMaster University under Animal Use Protocol #20-12-41. 6-8 week old, female BALB/c mice (Charles River Laboratories) were anesthetized using inhalant isoflurane. Buprenorphine (0.1 mg/kg) was administered intraperitoneally and eye gel was applied pre-procedure. A 2 cm^2 patch was clipped of hair on the dorsal surface and sterilized using a povidone-iodine wash. A plastic washer (6 mm inner diameter) was sutured in place and furthered glued down using Vetbond for reinforcement. A 5 mm diameter, full-thickness, excisional wound was created using a biopsy punch. Wounds were immediately infected with a bacterial inoculum of ~5x10^6 CFU *Staphylococcus*

aureus USA 300 suspended in PBS. The infection was left to establish for one hour prior to placement of treatment gel or disk.

The experimental period was 48 h, during which mice were monitored for wound bed humidity, weight change, and overall well-being at the 24 h and 48 h marks. Mice were euthanized at experimental endpoint of 48 h. Infected wound tissue and spleen samples were collected post-mortem, homogenized in phosphate buffered saline (PBS), and plated on LB plates supplemented with oxacillin to quantify bacterial loads.

Cyclophosphamide pre-treatment in mice

Mice were treated with CP in a two-dose regime on days T-4 and T-1 prior to infection. On day T-4, mice were weighed and injected with 150 mg/kg CP intraperitoneally. On day T-1, mice were weighed and injected with 100 mg/kg CP intraperitoneally. Mouse weight loss was monitored on both dosing days and daily throughout the infective period.

Fabrication of PGX polymer scaffold

A solution of sodium alginate (SA) and calcium chloride ($CaCl_2$) were pumped through a nozzle and mixed with the PGX fluid (SC-CO_2 and ethanol) at 40°C and 100 bar. The resulting precipitated, crosslinked SA (xSA) was then dried using SC-CO_2 to obtain a purified, dried fibrous aerogel (PGX-SA). This material was then mechanically compressed at 30 MPa to form a thin, porous film. 3/16-inch diameter disks, each

weighing ~4.5 mg, were then punched from the film using a hole-punch mechanism. Surface area measurements were conducted using gas sorption (~1 m^2 per disk)[38].

Supercritical loading of bioactive into polymer carrier

Approximately 10 mg of the drug of interest (FA or TIG) was saturated and solubilized within a stream of SC-CO_2 in a 10 mL, high-pressure vessel inside a 40°C chamber. The stream was then passed through a bed formed by the porous, PGX disks, allowing the drug to be adsorbed into the inner pores and surface area of the disks at an overall pressure of 200 bar. After 2 h of circulation, the vessel and its contents were depressurized, resulting in the SC-CO_2 converting to gaseous CO_2 and the remaining drug precipitating out of its solubilizing, supercritical carrier. This remaining drug was then precipitated onto the outer surface area of the PGX-SA disks[37].

PLA-POEGMA nanoparticle synthesis

PLA-$POEGMA_{475}$ block polymers were synthesized and filtered in preparation for nanoparticle fabrication using previously established protocols[43]. Three mL of acetone containing PLA-$POEGMA_{475}$ (10 mg/mL) was sonicated for approximately 1 h at room temperature. Fusidic acid (0.8 mg/mL) was added directly to the acetone/monomer solution for preparation of drug-containing SAPs. The slurry was loaded into one syringe and 3 mL MilliQ H_2O was loaded into a second syringe. The nanoparticles were then generated through flash nanoprecipitation using a 3D-printed, confined impinging jet mixer (CIJM) and a gas-pressurized pump. The entire contents of

both syringes were flash-mixed and released into a glass collection vial containing 3 mL MilliQ H_2O. The acetone solvent was evaporated overnight and the SAP suspension was collected via centrifugation (30 min, 50,000 x g, 15°C). The pellet was then resuspended in 2 mL MilliQ water in preparation for POEGMA gel loading.

POEGMA gel synthesis

Hydrazide- and aldehyde-functionalized POEGMA precursors were fabricated using previously established protocols[81]. SAP-containing POEGMA gels were fabricated using functionalized POEGMA monomers PO100H30 and PO100A30. The two monomers were diluted to a specified concentration (15 w/v%) using the SAP-MilliQ suspensions (drug-containing or blank). A one-to-one mixture of the two monomers was mixed and immediately pipetted into silicone molds (35 μL per 5.2 mm diameter mold). Gels were left to set in 4°C overnight (24 h before use). At time of wound placement, gels were extracted from the molds using a sterile spatula and MilliQ H_2O.

LC/MS drug loading quantification

Drug-impregnated PGX disks

Impregnated iPX disks were prepared for drug quantification by alginate degradation. Disks were dissolved in vials containing 6 mL 0.2M EDTA and 100 μL 0.1M alginate lyase for 30 min at 37°C. The hydrogel components were extracted via precipitation by concentrated HCl and centrifugation (2000 x g, 5 min). The drug-containing supernatant was isolated and drug was isolated using 3 replicate, 1 mL

dichloromethane extractions. Extraction layers were combined and evaporated under nitrogen before being resuspended in 1 mL acetonitrile containing 50 ng/mL FA-d6 or TIG-d9 (deuterated fusidic acid or tigecycline). Sampled were sonicated and vortexed for 1 min to ensure thorough mixing.

Samples were quantified using HPLC (Agilent 1290 Infinity II) and QQQ-MS (Agilent 6495C iFunnel) under the following experimental conditions. Separation was achieved with an analytical column (Agilent RRHD Eclipse Plus C_{18}): mobile phase – (A) 0.1% (v/v) formic acid in H_2O and (B) 0.1% (v/v) formic acid in acetonitrile, flow rate – 0.3 mL/min, temperature – 30°C. Separation specifications: linear gradient – 5% to 97% B over 7 min, held at 97% B for 0.5 min. Mass spectrometer: drying gas flow rate – 11L/min, drying gas temperature – 290°C, nebulizer pressure – 30 psi, sheath gas flow rate – 11L/min, sheath gas temperature – 300°C, capillary voltage – 2000V, nozzle voltage – 1500V, acquisition rate – 1.23 cycles/s.

SAP-containing POEGMA gels

POEGMA gels containing FA were soaked in 5 mL of simulated wound fluid (SWF), triggering dissolution of the drug particles from the polymer matrix. 500 μL samples were taken at time points ranging from T+1 hour to T+7 days. After each sample collection, a 500 μL aliquot of fresh SWF was replaced in the sample tube. A volume of 50 μL of each collected sample was loaded into a microcentrifuge tube. Two hundred μL of ice-cold acetonitrile + 0.1% formic acid and 62.5 ng/mL of fusidic acid-d6 was then added to each sample tube. The tubes were vortexed for 1 min and then centrifuged at

18,000 x g for 15 min to pellet the precipitated BSA. One hundred μL from the top of the sample was removed and diluted 100x with acetonitrile + 0.1% formic acid and 50 ng/mL fusidic acid-d6. Samples were prepared in triplicated and injected in duplicate.

Samples were quantified through HPLC (Agilent 1290 Infinity II) and QQQ-MS (Agilent 6495C iFunnel). Separation was achieved with an analytical column (Agilent RRHD Eclipse Plus C_{18}): mobile phase – (A) 0.1% (v/v) formic acid in H_2O and (B) 0.1% formic acid in acetonitrile, flow rate – 0.3 mL/min, temperature – 30°C. Separation specifications: linear gradient – 5% to 97% B over 7 min, held at 97% B for 0.5 min.

Electrospray ionization (ESI) was used for multiple reaction monitoring and quantification of analytes under the following specifications: drying gas flow rate – 11 L/min, drying gas temp. – 290°C, nebulizer pressure – 30 psig, sheath gas flow rate – 11 L/min, sheath gas temp. – 300°C, capillary voltage – 2000 V, nozzle voltage – 1500 V, acquisition rate – 1.23 cycles/sec, retention time – 8.46 min.

Figures

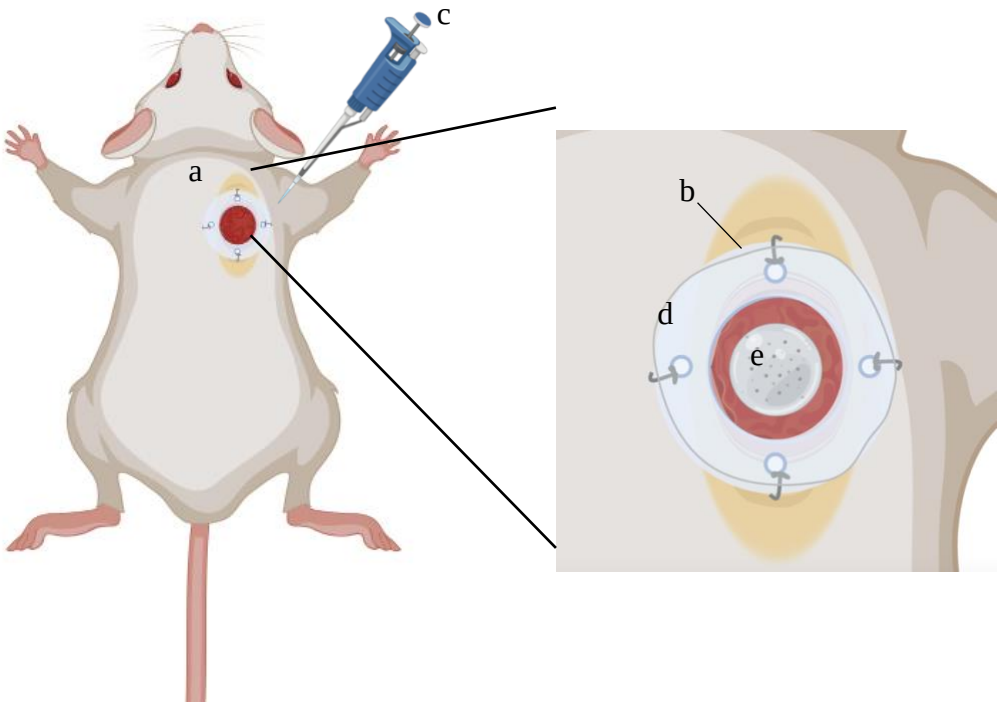

Figure 1: Full-thickness, murine skin-wound model of infection. After preparation (clipping) and sterilization of the dorsal surface, a 6mm excisional wound was created using a biopsy punch (a). To prevent wound contraction, a sterile plastic washer (6 mm inner diameter, 11 mm outer diameter) was fastened to the skin around the wound via suture and skin adhesive (Vetbond) (b). A prepared inoculum of bacteria was administered via pipetting directly into the wound site (c). A round adhesive film (Opsite, ~13 mm diameter) was used to cover the wound/washer area and entrap wound humidity (d). After 1 h the treatment disk or gel was placed inside the washer and wound area, under the adhesive layer (e). During harvesting, all necrotic and visibly infected tissue was extracted for post-mortem analyses.

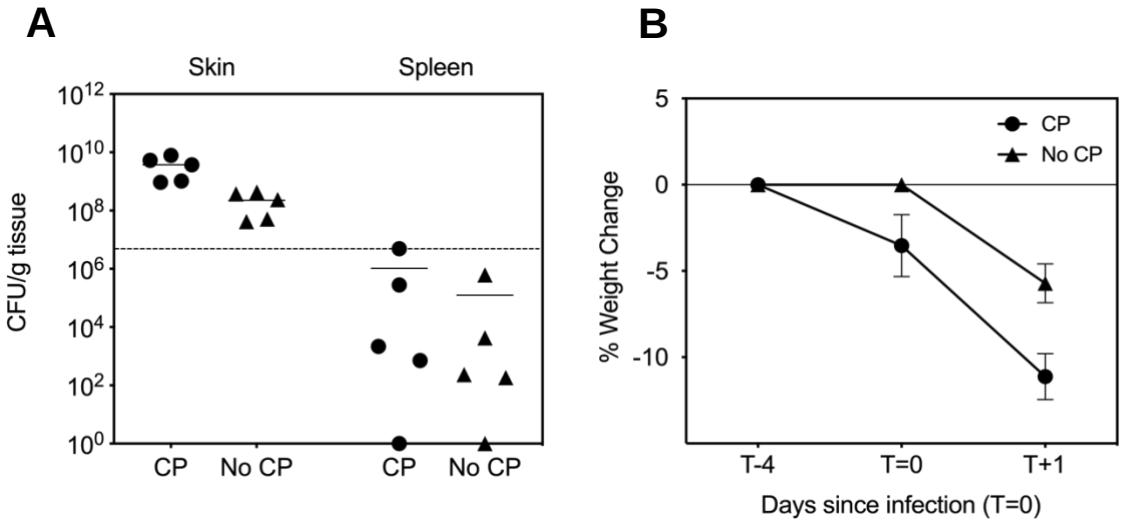

Figure 2: Cyclophosphamide pre-treatment is not necessary for establishing MRSA infection in mice. Female BALB/c mice, both pre-treated with CP (n=5, circle) or not pre-treated (n=5, triangle), were given full-thickness skin wounds inoculated with ~$5x10^6$ CFU MRSA (*S. aureus* Rosenbach, USA 300). Post-infection skin tissue and spleen bacterial counts were analyzed and expressed as CFU per gram tissue with the mean, along with starting inoculum dose (dashed, horizontal line) (A). Weight change was monitored on days T-4, T=0, and T+1, where T=0 represents the time of infection and T+1 represents the time of sacrifice. Weight change is represented as average % body weight lost since previous point of measurement for each group, along with standard error of the mean (SEM) (B). These data represents two independent replicates, one of 2 mice per group and another of 3 mice per group.

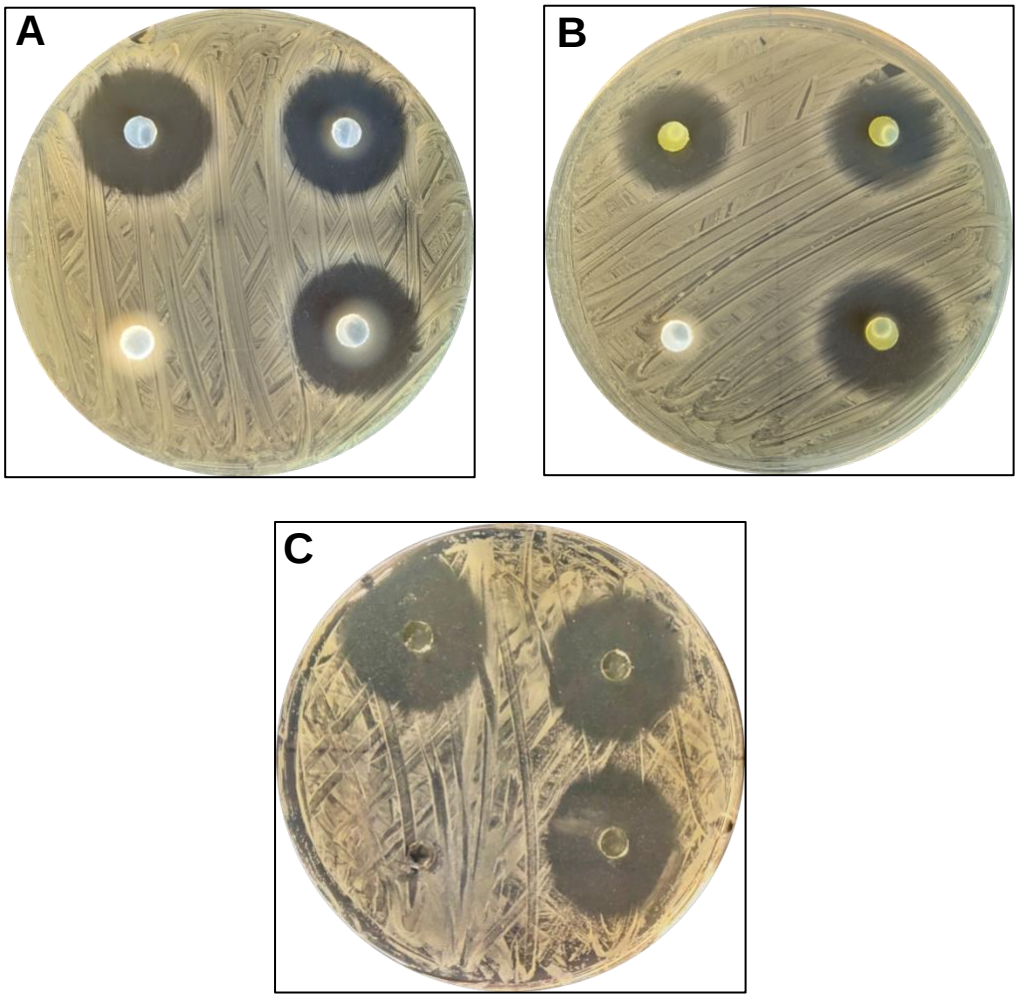

Figure 3: Disk-diffusion assays reveal FA- and TIG-iPX disks and FA-POEGMA gels are homogenously loaded. iPX disks impregnated with FA (A) and TIG (B) and POEGMA gels containing FA-SAPs (C) were placed in triplicate on agar plates inoculated with MRSA (*S. aureus* Rosenbach, USA 300). Each plate contained one blank control disk or gel, shown in the lower-left corner on each image. The plates were incubated for 16-18 hr at 37°C and before being evaluated and imaged.

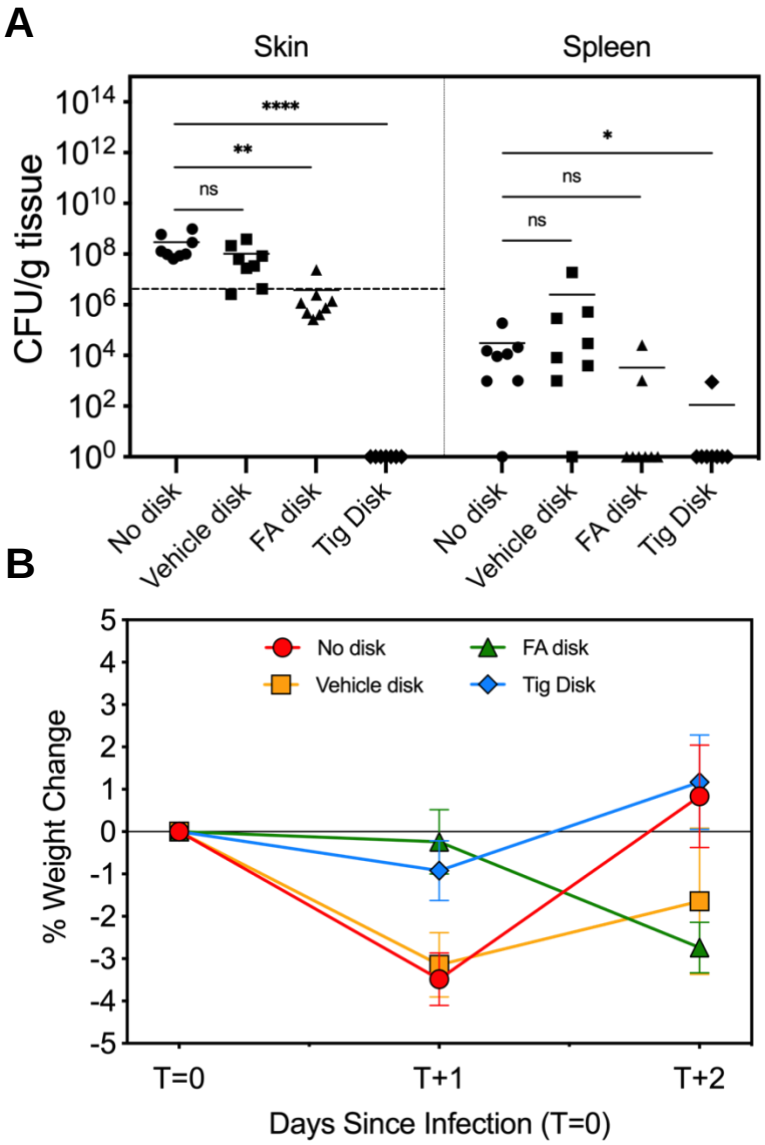

Figure 4: Drug-impregnated iPX disks reduce MRSA wound colonization. Female, BALB/c mice were subjected to the full thickness wound procedure mentioned previously, and inoculated topically with ~5x10^6 CFU MRSA (*S. aureus* Rosenbach, USA 300). Mice received either no disk (circle), vehicle PGX disks (square), FA-iPX disks (triangle), TIG-iPX disks (diamond), or FA-AZT-iPX disks (open circle), 1 h after

inoculation. After 48 h, bacterial colonization was evaluated in infected skin tissue and spleen samples and is expressed in CFU/g tissue along with the mean (A). Dashed horizontal line represents inoculum dose. Weight change and animal condition was monitored daily and represented by average % body weight change since previous time point for each group, with SEM (B). These data represent two independent experiments for each treatment group, with n=8 for each group. Statistical significance was determined using a non-parametric Kruskal-Wallis test (ns-no significance, *$P<0.05$, **$P<0.01$, ***$P<0.001$).

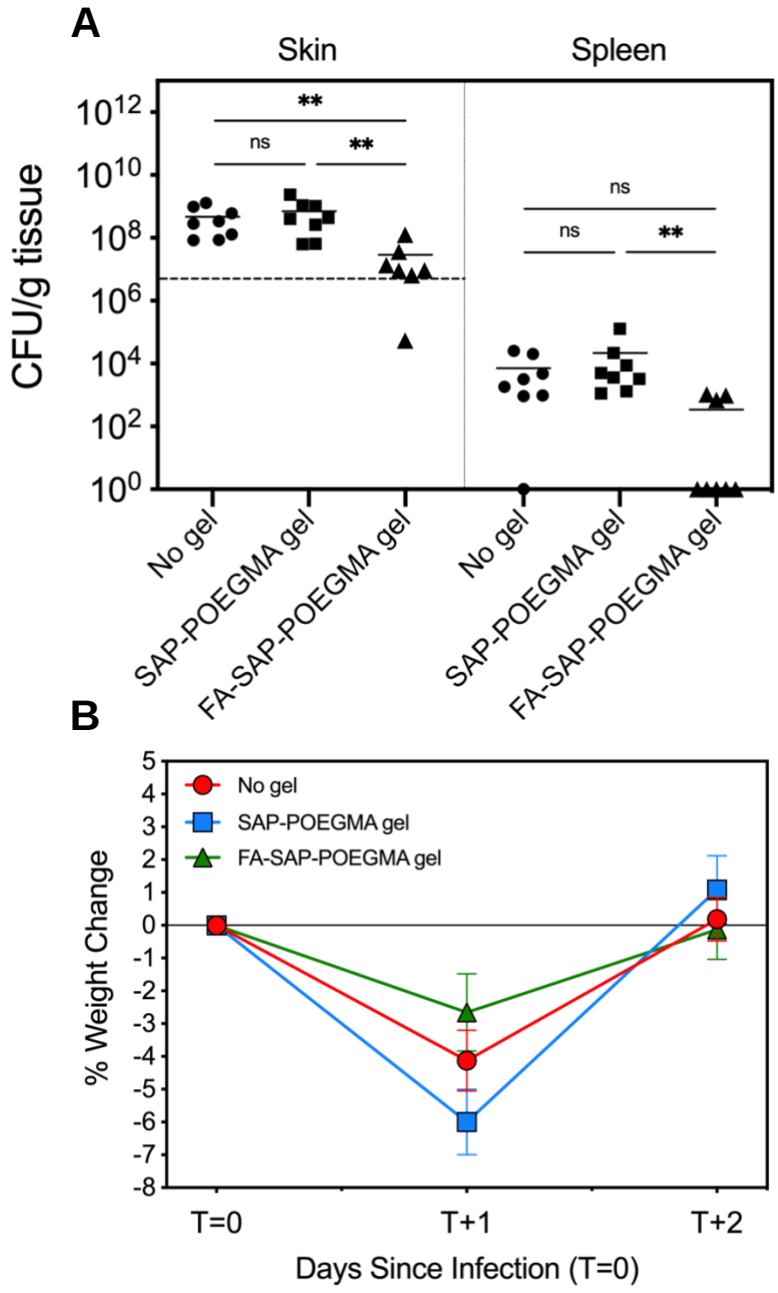

Figure 5: FA-SAP-containing POEGMA gels reduce MRSA wound colonization. Female BALB/c mice were subjected to a full thickness wound procedure and inoculated topically with ~5x10^6 CFU MRSA (*S. aureus* Rosenbach, USA 300). Mice received either no gel (circle), drug-free SAP-POEGMA gels (square), or FA-POEGMA gels

(triangle), 1 h after inoculation. After a 48 h treatment period, bacterial colonization was evaluated in infected skin tissue and spleen samples and is expressed in CFU/g tissue along with the mean (A). Dashed horizontal line represents inoculum dose. Weight change and animal condition was monitored daily and is represented by average % body weight lost since previous time point for each group, with SEM (B). Thesse data represent one independent experiment for each treatment group, with n=8 for each group. Statistical significance was determined using a non-parametric Kruskal-Wallis test (ns-no significance, *P<0.05, **P<0.01, ***P<0.001).

A

Sample ID	Spike Level	FA % Recovery
QC1	20 µg	49%
QC2	20 µg	50%
QC3	20 µg	43%
	Average	**47%**
	SD	**3%**

B

Sample ID	Description	Amount FA (mg)*
Disk 1	Hydrogel disk 1, weight 4.6 mg	0.0049
Disk 2	Hydrogel disk 2, weight 4.4 mg	0.0057
Disk 3	Hydrogel disk 3, weight 3.7 mg	0.0046
	Average	**0.0051**

***Amount has been adjusted to account for 47% recovery.**

Figure 6: HPLC/MS quantifies drug-loading levels of iPX disks. Triplicate control samples were used to prepare a standard curve to estimate FA recovery by the LC/MS protocol used. Three 20 µg-spiked samples were measured and FA recovery is expressed as % of total spike amount, with average and standard deviation (A). Triplicate FA-iPX disks were then prepared and analyzed for loading amounts. Data are represented as total amount FA detected per disk, adjusted to account for 47% recovery levels in QC trials, with average (B).

References

1. Sawyer RG, Pruett TL. Wound infections. *Surg Clin North Am*. 1994;74(3):519-536. doi:10.1016/s0039-6109(16)46327-9

2. Falcone M, De Angelis B, Pea F, et al. Challenges in the management of chronic wound infections. *J Glob Antimicrob Resist*. 2021;26:140-147. doi:10.1016/j.jgar.2021.05.010

3. Guo S, DiPietro LA. Factors Affecting Wound Healing. *J Dent Res*. 2010;89(3):219-229. doi:10.1177/0022034509359125

4. Menke NB, Ward KR, Witten TM, Bonchev DG, Diegelmann RF. Impaired wound healing. *Clin Dermatol*. 2007;25(1):19-25. doi:10.1016/j.clindermatol.2006.12.005

5. Robson MC, Stenberg BD, Heggers JP. Wound Healing Alterations Caused by Infection. *Clin Plast Surg*. 1990;17(3):485-492. doi:10.1016/S0094-1298(20)30623-4

6. Naskar A, Kim K sun. Recent Advances in Nanomaterial-Based Wound-Healing Therapeutics. *Pharmaceutics*. 2020;12(6):499. doi:10.3390/pharmaceutics12060499

7. De Brabandere K, Jacobs-Tulleneers-Thevissen D, Czapla J, La Meir M, Delvaux G, Wellens F. Negative-Pressure Wound Therapy and Laparoscopic Omentoplasty for Deep Sternal Wound Infections after Median Sternotomy. *Tex Heart Inst J*. 2012;39(3):367-371.

8. El-Ashram S, El-Samad LM, Basha AA, El Wakil A. Naturally-derived targeted therapy for wound healing: Beyond classical strategies. *Pharmacol Res*. 2021;170:105749. doi:10.1016/j.phrs.2021.105749

9. Kaiser P, Wächter J, Windbergs M. Therapy of infected wounds: overcoming clinical challenges by advanced drug delivery systems. *Drug Deliv Transl Res*. 2021;11(4):1545-1567. doi:10.1007/s13346-021-00932-7

10. Sen CK. Human Wounds and Its Burden: An Updated Compendium of Estimates. *Adv Wound Care*. 2019;8(2):39-48. doi:10.1089/wound.2019.0946

11. Yao Z, Niu J, Cheng B. Prevalence of Chronic Skin Wounds and Their Risk Factors in an Inpatient Hospital Setting in Northern China. *Adv Skin Wound Care*. 2020;33(9):1-10. doi:10.1097/01.ASW.0000694164.34068.82

12. Mayon-White RT, Ducel G, Kereselidze T, Tikomirov E. An international survey of the prevalence of hospital-acquired infection. *J Hosp Infect*. 1988;11:43-48. doi:10.1016/0195-6701(88)90164-8

13. Hurd T, Posnett J. Point prevalence of wounds in a sample of acute hospitals in Canada. *Int Wound J*. 2009;6(4):287-293. doi:10.1111/j.1742-481X.2009.00615.x

14. Insights FB. Wound Care Market to Hit USD 24.01 Billion by 2028 with 6.1% CAGR | Market Size, Share, Growth, Forecasts, & Trends Analysis Report with COVID-19 Impact by Fortune Business Insights™. GlobeNewswire News Room. Published November 2, 2021. Accessed June 28, 2022. https://www.globenewswire.com/news-release/2021/11/02/2325048/0/en/Wound-Care-Market-to-Hit-USD-24-01-Billion-by-2028-with-6-1-CAGR-Market-Size-Share-Growth-Forecasts-Trends-Analysis-Report-with-COVID-19-Impact-by-Fortune-Business-Insights.html

15. McArthur AG, Wright GD. Bioinformatics of antimicrobial resistance in the age of molecular epidemiology. *Curr Opin Microbiol*. 2015;27:45-50. doi:10.1016/j.mib.2015.07.004

16. Tacconelli E, N. Magrini. GLOBAL PRIORITY LIST OF ANTIBIOTIC-RESISTANT BACTERIA TO GUIDE RESEARCH, DISCOVERY, AND DEVELOPMENT OF NEW ANTIBIOTICS. :7.

17. Mulani MS, Kamble EE, Kumkar SN, Tawre MS, Pardesi KR. Emerging Strategies to Combat ESKAPE Pathogens in the Era of Antimicrobial Resistance: A Review. *Front Microbiol*. 2019;10:539. doi:10.3389/fmicb.2019.00539

18. Marston HD, Dixon DM, Knisely JM, Palmore TN, Fauci AS. Antimicrobial Resistance. *JAMA*. 2016;316(11):1193-1204. doi:10.1001/jama.2016.11764

19. Enright MC, Robinson DA, Randle G, Feil EJ, Grundmann H, Spratt BG. The evolutionary history of methicillin-resistant Staphylococcus aureus (MRSA). *Proc Natl Acad Sci*. 2002;99(11):7687-7692. doi:10.1073/pnas.122108599

20. Kaur DC, Chate SS. Study of Antibiotic Resistance Pattern in Methicillin Resistant Staphylococcus Aureus with Special Reference to Newer Antibiotic. *J Glob Infect Dis*. 2015;7(2):78-84. doi:10.4103/0974-777X.157245

21. Adhya A, Bain J, Ray O, et al. Healing of burn wounds by topical treatment: A randomized controlled comparison between silver sulfadiazine and nano-crystalline silver. *J Basic Clin Pharm*. 2014;6(1):29-34. doi:10.4103/0976-0105.145776

22. Savjani KT, Gajjar AK, Savjani JK. Drug Solubility: Importance and Enhancement Techniques. *ISRN Pharm*. 2012;2012:195727. doi:10.5402/2012/195727

23. Williams HD, Trevaskis NL, Charman SA, et al. Strategies to address low drug solubility in discovery and development. *Pharmacol Rev*. 2013;65(1):315-499. doi:10.1124/pr.112.005660

24. Godtfredsen WO, Jahnsen S, Lorck H, Roholt K, Tybring L. Fusidic Acid: a New Antibiotic. *Nature*. 1962;193. Accessed June 24, 2022. https://www.cabdirect.org/cabdirect/abstract/19622704146

25. Curbete MM, Salgado HRN. A Critical Review of the Properties of Fusidic Acid and Analytical Methods for Its Determination. *Crit Rev Anal Chem*. 2016;46(4):352-360. doi:10.1080/10408347.2015.1084225

26. Wenzel R, Bate G, Kirkpatrick P. Tigecycline. *Nat Rev Drug Discov*. 2005;4(10):809-810. doi:10.1038/nrd1857

27. Chopra I. Glycylcyclines: third-generation tetracycline antibiotics. *Curr Opin Pharmacol*. 2001;1(5):464-469. doi:10.1016/S1471-4892(01)00081-9

28. Greer ND. Tigecycline (Tygacil): the first in the glycylcycline class of antibiotics. *Proc Bayl Univ Med Cent*. 2006;19(2):155-161.

29. Simonetti O, Cirioni O, Lucarini G, et al. Tigecycline accelerates staphylococcal-infected burn wound healing through matrix metalloproteinase-9 modulation. *J Antimicrob Chemother*. 2012;67(1):191-201. doi:10.1093/jac/dkr440

30. Bassetti M, Nicolini L, Repetto E, Righi E, Del Bono V, Viscoli C. Tigecycline use in serious nosocomial infections: a drug use evaluation. *BMC Infect Dis*. 2010;10:287. doi:10.1186/1471-2334-10-287

31. Goktas S, Kurtoglu MG, Sakarya Y, et al. New Therapy Option for Treatment of Methicillin-Resistant Staphylococcus aureus Keratitis: Tigecycline. *J Ocul Pharmacol Ther*. 2015;31(2):122-127. doi:10.1089/jop.2014.0052

32. Nimal TR, Baranwal G, Bavya MC, Biswas R, Jayakumar R. Anti-staphylococcal Activity of Injectable Nano Tigecycline/Chitosan-PRP Composite Hydrogel Using Drosophila melanogaster Model for Infectious Wounds. *ACS Appl Mater Interfaces*. 2016;8(34):22074-22083. doi:10.1021/acsami.6b07463

33. Sakarya Y, Sakarya R, Ozcimen M, et al. Ocular penetration of topically applied 1% tigecycline in a rabbit model. *Int J Ophthalmol*. 2017;10(5):679-683. doi:10.18240/ijo.2017.05.03

34. Breedt J, Teras J, Gardovskis J, et al. Safety and Efficacy of Tigecycline in Treatment of Skin and Skin Structure Infections: Results of a Double-Blind Phase 3 Comparison Study with Vancomycin-Aztreonam. *Antimicrob Agents Chemother*. 2005;49(11):4658-4666. doi:10.1128/AAC.49.11.4658-4666.2005

35. Agwuh KN, MacGowan A. Pharmacokinetics and pharmacodynamics of the tetracyclines including glycylcyclines. *J Antimicrob Chemother*. 2006;58(2):256-265. doi:10.1093/jac/dkl224

36. Boateng JS, Matthews KH, Stevens HNE, Eccleston GM. Wound Healing Dressings and Drug Delivery Systems: A Review. *J Pharm Sci*. 2008;97(8):2892-2923. doi:10.1002/jps.21210

37. Temelli F, Seifried B. Supercritical fluid treatment of high molecular weight biopolymers. Published online February 2, 2016. Accessed June 28, 2022. https://patents.google.com/patent/US9249266B2/en

38. Liu Z, Couto R, Seifried B, Yépez B, Moquin P, Temelli F. Drying of sodium alginate using Pressurized Gas eXpanded (PGX) liquid technology. *J CO2 Util*. 2022;61:102006. doi:10.1016/j.jcou.2022.102006

39. Duarte ARC, Simplicio AL, Vega-González A, et al. Supercritical fluid impregnation of a biocompatible polymer for ophthalmic drug delivery. *J Supercrit Fluids*. 2007;42(3):373-377. doi:10.1016/j.supflu.2007.01.007

40. Couto R, Seifried B, Yépez B, Moquin P, Temelli F. Adsorptive precipitation of co-enzyme Q10 on PGX-processed β-glucan powder. *J Supercrit Fluids*. 2018;141:157-165. doi:10.1016/j.supflu.2017.12.016

41. Francesko A, Petkova P, Tzanov T. Hydrogel Dressings for Advanced Wound Management. *Curr Med Chem*. 2019;25(41):5782-5797. doi:10.2174/0929867324666170920161246

42. Su J, Li J, Liang J, Zhang K, Li J. Hydrogel Preparation Methods and Biomaterials for Wound Dressing. *Life*. 2021;11(10):1016. doi:10.3390/life11101016

43. Emilia B, Niels S, Spencer I, Todd H. Injectable and degradable Poly(oligoethylene glycol methacrylate)-based hydrogels-synthetic versatility for improved biomaterial design. *Front Bioeng Biotechnol*. 2016;4. doi:10.3389/conf.FBIOE.2016.01.00622

44. Manepalli S, Gandhi JA, Ekhar VV, Asplund MB, Coelho C, Martinez LR. Characterization of a cyclophosphamide-induced murine model of immunosuppression to study Acinetobacter baumannii pathogenesis. *J Med Microbiol*. 2013;62(Pt 11):1747-1754. doi:10.1099/jmm.0.060004-0

45. Ren Z, Laumann AE, Silverberg JI. Association of dermatomyositis with systemic and opportunistic infections in the United States. *Arch Dermatol Res*. 2019;311(5):377-387. doi:10.1007/s00403-019-01913-0

46. Zuluaga AF, Salazar BE, Rodriguez CA, Zapata AX, Agudelo M, Vesga O. Neutropenia induced in outbred mice by a simplified low-dose cyclophosphamide regimen: characterization and applicability to diverse experimental models of infectious diseases. *BMC Infect Dis*. 2006;6:55. doi:10.1186/1471-2334-6-55

47. Davidson JM, Yu F, Opalenik SR. Splinting Strategies to Overcome Confounding Wound Contraction in Experimental Animal Models. *Adv Wound Care*. 2013;2(4):142-148. doi:10.1089/wound.2012.0424

48. May A, Kopecki Z, Carney B, Cowin A. Antimicrobial silver dressings: a review of emerging issues for modern wound care. *ANZ J Surg*. 2022;92(3):379-384. doi:10.1111/ans.17382

49. Gupta P, Vermani K, Garg S. Hydrogels: from controlled release to pH-responsive drug delivery. *Drug Discov Today*. 2002;7(10):569-579. doi:10.1016/s1359-6446(02)02255-9

50. Prabaharan M, Mano JF. Stimuli-Responsive Hydrogels Based on Polysaccharides Incorporated with Thermo-Responsive Polymers as Novel Biomaterials. *Macromol Biosci*. 2006;6(12):991-1008. doi:10.1002/mabi.200600164

51. Singh B, Sharma S, Dhiman A. Design of antibiotic containing hydrogel wound dressings: Biomedical properties and histological study of wound healing. *Int J Pharm*. 2013;457(1):82-91. doi:10.1016/j.ijpharm.2013.09.028

52. Song A, Rane AA, Christman KL. Antibacterial and cell-adhesive polypeptide and poly(ethylene glycol) hydrogel as a potential scaffold for wound healing. *Acta Biomater*. 2012;8(1):41-50. doi:10.1016/j.actbio.2011.10.004

53. Harries RL, Bosanquet DC, Harding KG. Wound bed preparation: TIME for an update. *Int Wound J*. 2016;13(S3):8-14. doi:10.1111/iwj.12662

54. Jain S, Domb AJ, Kumar N. Drug Delivery to Wounds, Burns, and Diabetes-Related Ulcers. In: Domb AJ, Khan W, eds. *Focal Controlled Drug Delivery*. Advances in Delivery Science and Technology. Springer US; 2014:585-605. doi:10.1007/978-1-4614-9434-8_26

55. Adepu S, Ramakrishna S. Controlled Drug Delivery Systems: Current Status and Future Directions. *Molecules*. 2021;26(19):5905. doi:10.3390/molecules26195905

56. Winter GD. Formation of the Scab and the Rate of Epithelization of Superficial Wounds in the Skin of the Young Domestic Pig. *Nature*. 1962;193(4812):293-294. doi:10.1038/193293a0

57. Seifried B, Temelli F, Vine D, et al. PGX TECHNOLOGY: NOVEL TAILOR-MADE AND TUNEABLE DELIVERY SYSTEMS FOR POORLY WATER-SOLUBLE BIOACTIVES. In: ; 2019. doi:10.24355/dbbs.084-202001221507-0

58. Globale P, Kumar A, Sahoo S, et al. REVIEW ON SOLUBILITY ENHANCEMENT TECHNIQUES FOR HYDROPHOBIC DRUGS. 2011;3.

59. Blagden N, de Matas M, Gavan PT, York P. Crystal engineering of active pharmaceutical ingredients to improve solubility and dissolution rates. *Adv Drug Deliv Rev*. 2007;59(7):617-630. doi:10.1016/j.addr.2007.05.011

60. Dubey R. Impact of Nanosuspension Technology on Drug Discovery & Development. *Drug Deliv Technol*. 2006;6.

61. Chaumeil JC. Micronization: a method of improving the bioavailability of poorly soluble drugs. *Methods Find Exp Clin Pharmacol*. 1998;20(3):211-215.

62. Vogt M, Kunath K, Dressman JB. Dissolution enhancement of fenofibrate by micronization, cogrinding and spray-drying: comparison with commercial preparations. *Eur J Pharm Biopharm Off J Arbeitsgemeinschaft Pharm Verfahrenstechnik EV*. 2008;68(2):283-288. doi:10.1016/j.ejpb.2007.05.010

63. Chiou WL, Riegelman S. Pharmaceutical applications of solid dispersion systems. *J Pharm Sci*. 1971;60(9):1281-1302. doi:10.1002/jps.2600600902

64. Leuenberger H. Spray Freeze-drying – The Process of Choice for Low Water Soluble Drugs? *J Nanoparticle Res*. 2002;4(1):111-119. doi:10.1023/A:1020135603052

65. Lutz JF, Hoth A. Preparation of Ideal PEG Analogues with a Tunable Thermosensitivity by Controlled Radical Copolymerization of 2-(2-Methoxyethoxy)ethyl Methacrylate and Oligo(ethylene glycol) Methacrylate. *Macromolecules*. 2006;39(2):893-896. doi:10.1021/ma0517042

66. Wang XS, Armes SP. Facile Atom Transfer Radical Polymerization of Methoxy-Capped Oligo(ethylene glycol) Methacrylate in Aqueous Media at Ambient Temperature. *Macromolecules*. 2000;33(18):6640-6647. doi:10.1021/ma000671h

67. Rafat M, Cléroux CA, Fong WG, et al. PEG–PLA microparticles for encapsulation and delivery of Tat-EGFP to retinal cells. *Biomaterials*. 2010;31(12):3414-3421. doi:10.1016/j.biomaterials.2010.01.031

68. Hu Z, Cai T, Chi C. Thermoresponsive oligo(ethylene glycol)-methacrylate- based polymers and microgels. *Soft Matter*. 2010;6(10):2115-2123. doi:10.1039/B921150K

69. Bauer AW, Kirby WMM, Sherris JC, Turck M. Antibiotic Susceptibility Testing by a Standardized Single Disk Method. *Am J Clin Pathol*. 1966;45(4_ts):493-496. doi:10.1093/ajcp/45.4_ts.493

70. Craig W. Relevance of animal models for clinical treatment. *Eur J Clin Microbiol Infect Dis*. 1993;12(1):S55-S57. doi:10.1007/BF02389879

71. Zak O, Tosch W, Sande MA. Correlation of antibacterial activities of antibiotics in vitro and in animal models of infection. *J Antimicrob Chemother*. 1985;15 Suppl A:273-282. doi:10.1093/jac/15.suppl_a.273

72. Tuomanen E, Durack DT, Tomasz A. Antibiotic tolerance among clinical isolates of bacteria. *Antimicrob Agents Chemother*. 1986;30(4):521-527.

73. Kugelberg E, Norström T, Petersen TK, Duvold T, Andersson DI, Hughes D. Establishment of a Superficial Skin Infection Model in Mice by Using Staphylococcus aureus and Streptococcus pyogenes. *Antimicrob Agents Chemother*. 2005;49(8):3435-3441. doi:10.1128/AAC.49.8.3435-3441.2005

74. Hankenson FC, Ruskoski N, van Saun M, Ying GS, Oh J, Fraser NW. Weight loss and reduced body temperature determine humane endpoints in a mouse model of ocular herpesvirus infection. *J Am Assoc Lab Anim Sci JAALAS*. 2013;52(3):277-285.

75. Marcus Y. Are solubility parameters relevant to supercritical fluids? *J Supercrit Fluids*. 2006;38(1):7-12. doi:10.1016/j.supflu.2005.11.008

76. Ganesh K, Sinha M, Mathew-Steiner SS, Das A, Roy S, Sen CK. Chronic Wound Biofilm Model. *Adv Wound Care*. 2015;4(7):382-388. doi:10.1089/wound.2014.0587

77. Dalton T, Dowd SE, Wolcott RD, et al. An in vivo polymicrobial biofilm wound infection model to study interspecies interactions. *PloS One*. 2011;6(11):e27317. doi:10.1371/journal.pone.0027317

78. Dai T, Tegos GP, Zhiyentayev T, Mylonakis E, Hamblin MR. Photodynamic therapy for methicillin-resistant *Staphylococcus aureus* infection in a mouse skin abrasion model: PHOTODYNAMIC THERAPY FOR MRSA. *Lasers Surg Med*. 2010;42(1):38-44. doi:10.1002/lsm.20887

79. Park JE, Barbul A. Understanding the role of immune regulation in wound healing. *Am J Surg*. 2004;187(5, Supplement 1):S11-S16. doi:10.1016/S0002-9610(03)00296-4

80. Pierce GF, Mustoe TA, Lingelbach J, Masakowski VR, Gramates P, Deuel TF. Transforming growth factor beta reverses the glucocorticoid-induced wound-healing deficit in rats: possible regulation in macrophages by platelet-derived growth factor. *Proc Natl Acad Sci U S A*. 1989;86(7):2229-2233. doi:10.1073/pnas.86.7.2229

81. Bakaic E, Smeets NMB, Hoare T. Injectable hydrogels based on poly(ethylene glycol) and derivatives as functional biomaterials. *RSC Adv*. 2015;5(45):35469-35486. doi:10.1039/C4RA13581D

Appendix

Methods

Fabrication and *in vitro* testing of thiostrepton (TS) and fusidic acid/azidothymidine (FA/AZT)-iPX disks

PGX-SA material was generated and impregnated with TS or FA as previously described. FA-iPX disks were soaked in a 20 mg/mL solution of azidothymidine (AZT) in MilliQ H_2O for 10 seconds prior to placement onto plate. Treatment disks were placed in triplicate on LB-agar plates inoculated with MRSA (*S. aureus* Rosenbach strain USA 300), along with a control (blank) disk. Plates were inoculated at 37°C for 16-18 hours. Zones of growth inhibition were qualitatively examined to anticipate successful drug diffusion from iPX disks *in vivo*.

In vivo testing of TS and FA/AZT disks

The excisional wound model was carried out as previously described for both TS and FA/AZT iPX disks on 6-8 w/o female, BALB/c mice (Charles River Laboratories). FA-iPX disks were soaked in a 20 mg/mL solution of AZT in MilliQ H_2O for 10 seconds prior to placement into infected wounds. Infected skin tissue and spleen samples were harvested post-mortem for bacterial CFU quantification. Weight change was monitored during the course of the infective/treatment period.

MRSA growth curves

TIG collected from the SC-AP vessel post-impregnation (iTIG) was evaluated for loss of activity as compared to standard, purified TIG. An overnight culture of MRSA (S. aureus Rosenbach strain USA 300) grown and subcultured 1:500 in 15 mL LB. 100 μL of the subculture was added to columns 2-11 in a 96-well plate. 256 μg/mL stocks were prepared of sodium fusidate (SF), oxacillin (OX), TIG, and iTIG using the subcultured MRSA in LB. 200 μL of each compound stock was added to column 1 of different rows on the 96-well plate. A serial dilution was carried out between rows 1 and 11, resulting in antibiotic concentrations ranging from 256 μg/mL to 0.25 μg/mL. Column 12 was used as a blank and contained no antibiotic or bacteria. The plate was read using an Epoch Microplate Spectrophotometer and BioTek Gen5 software under the following protocol: shaking incubation at 37°C for 24 hrs, OD_{600} measurement taken every 30 min.

Results

***In vitro* tests show successful loading and deposition of TS and FA/AZT by iPX disks**

The same disk diffusion assays introduced previously were utilized to determine loading success of TS and FA/AZT disks. Both products displayed successful and near-homogenous loading of antibiotics compounds as evident by consistent zones of inhibition between treatment disks (**Figure 7**). TS iPX disks had an average inhibitory zone diameter of 23 mm and FA/AZT disks had an average inhibitory zone diameter of 24.7 mm.

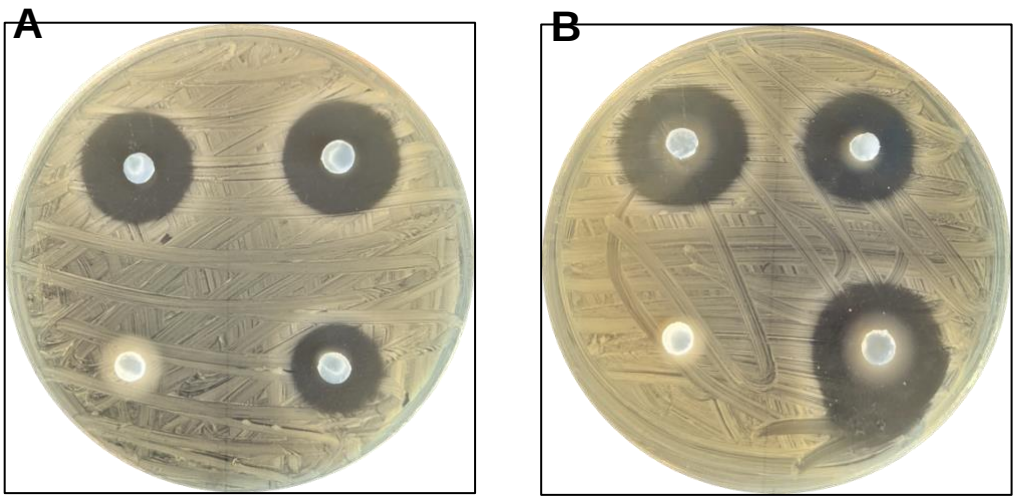

Figure 7: Disk-diffusion assays reveal TS- and FA/AZT-iPX disks are homogenously loaded. iPX disks impregnated with TS (A) and FA/AZT (B) were placed in triplicate on agar plates inoculated with MRSA (*S. aureus* Rosenbach, USA 300). Each plate contained one blank control disk, shown in the lower-left corner on each image. The plates were incubated for 16-18 hr at 37°C and before being evaluated and imaged.

Neither TS- nor FA/AZT-iPX disks effectively prevent MRSA colonization *in vivo*

The full-thickness skin wound model previously introduced was utilized to evaluate success of TS- and FA/AZT-iPX disks as drug delivery vehicles in compromised wounds. Treatment disks were placed in wound beds 1hr post-infection (~$5x10^6$ CFU inoculum) and left to deposit drug for 48 hours. Both disks were unsuccessful in preventing the colonization of MRSA in the wound. Mice that received the TS-iPX disks displayed similar wound CFU counts to those receiving the vehicle disks (TS mean:

$6.6x10^7$ CFU, vehicle mean: $1.0x10^8$ CFU). Mice that received the FA/AZT-iPX disks had near-identical wound CFU counts to untreated mice (FA/AZT mean: $3.0x10^8$ CFU, untreated mean: $2.9x10^8$ CFU). There is no significance between any skin tissue data sets or spleen data sets (**Figure 8**). .

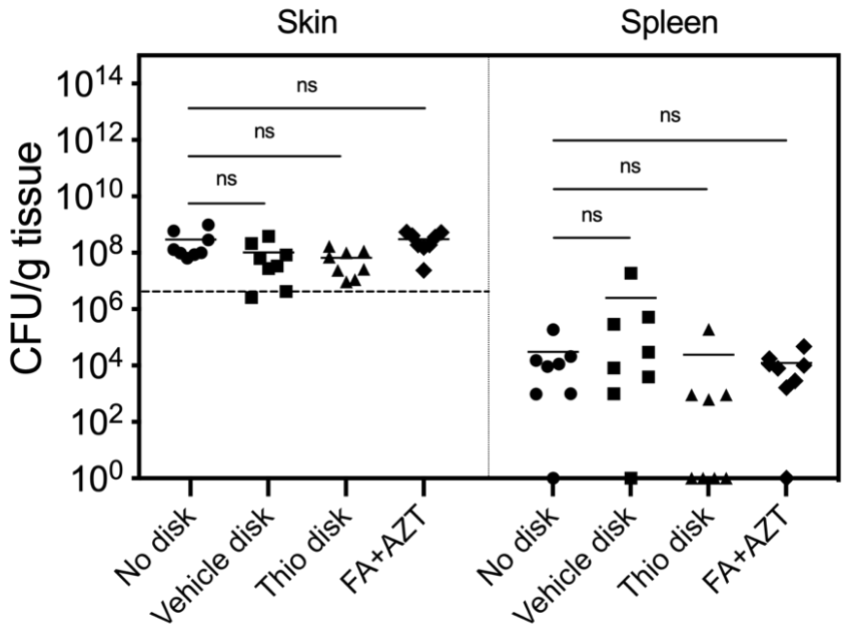

Figure 8: *In vivo* model results suggest TS- and FA/AZT-impregnated iPX disks are unsuccessful in preventing MRSA wound colonization. Female, BALB/c mice were subjected to the full thickness wound procedure mentioned previously, and inoculated topically with ~$5x10^6$ CFU MRSA (*S. aureus* Rosenbach, USA 300). Mice received either no disk (circle), vehicle PGX disks (square), TS-iPX disks (triangle), or FA/AZT-iPX disks (diamond), one hour after inoculation. After a 48hr treatment period, bacterial colonization was evaluated in infected skin tissue and spleen samples and is expressed in CFU/g tissue along with the mean (A). Dashed horizontal line represents inoculum dose.

This data represents independent experiments for each treatment group, with n=8 for each group. Statistical significance was determined using a non-parametric Kruskal-Wallis test (ns-no significance, *P<0.05, **P<0.01, ***P<0.001).

SC-AP processing and solubilization does not alter the activity of, or destabilize TIG.

A 24-hour growth curve was used to evaluate activity differences between standard and processed TIG. MRSA growth curves under TIG MIC and sub-MIC concentrations (0.5 and 0.25 μg/mL, respectively) exhibit no difference in level or trajectory of expansion. At a concentration of 0.25 μg/mL for both TIG and iTIG, the MRSA culture enters its exponential phase at around 12 hours. At a concentration of 0.5 μg/mL, both cultures undergo no expansion during the entirety of the experiment. These results preliminarily suggests that there are no discernable, qualitative differences in antibiotic activity between TIG and SC-AP-processed TIG.

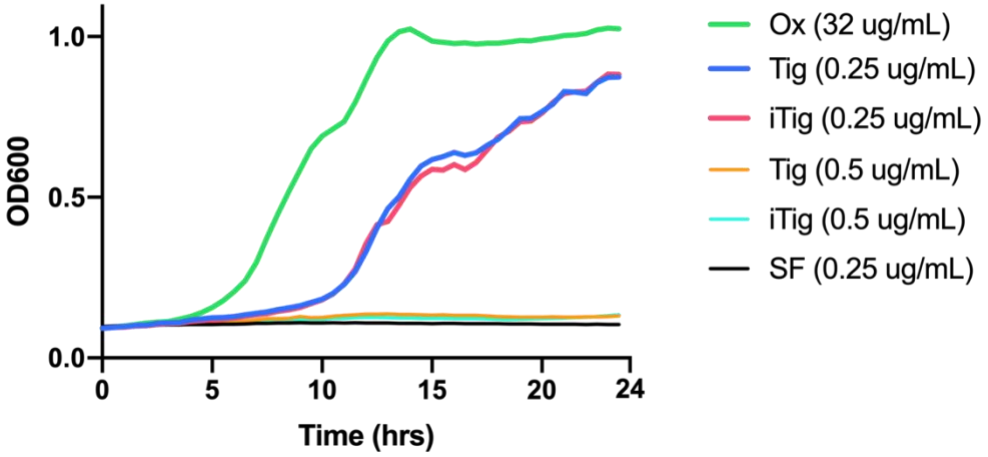

Figure 9: Growth curves reveal SC-AP solubilization and impregnation has no destabilizing effects on TIG. A 24-hour growth curve was used to evaluate antibiotic effects on a liquid MRSA culture. OD_{600} measurements of cultures containing OX (green), TIG (dark blue and orange), iTIG (red and light blue), and SF (black) at various concentrations are shown as a function of time. SF and OX were used as positive and negative controls, respectively.